nature communications

Article

https://doi.org/10.1038/s41467-025-57327-2

High-order Michaelis-Menten equations allow inference of hidden kinetic parameters in enzyme catalysis

Received: 12 June 2024

Accepted: 11 February 2025

Published online: 20 March 2025

Check for updates

Divya Singh[1], Tal Robin[2], Michael Urbakh[1] & Shlomi Reuveni[1]

Single-molecule measurements provide a platform for investigating the dynamical properties of enzymatic reactions. To this end, the single-molecule Michaelis-Menten equation was instrumental as it asserts that the first moment of the enzymatic turnover time depends linearly on the reciprocal of the substrate concentration. This, in turn, provides robust and convenient means to determine the maximal turnover rate and the Michaelis-Menten constant. Yet, the information provided by these parameters is incomplete and does not allow access to key observables such as the lifetime of the enzyme-substrate complex, the rate of substrate-enzyme binding, and the probability of successful product formation. Here we show that these quantities and others can be inferred via a set of high-order Michaelis-Menten equations that we derive. These equations capture universal linear relations between the reciprocal of the substrate concentration and distinguished combinations of turnover time moments, essentially generalizing the Michaelis-Menten equation to moments of any order. We demonstrate how key observables such as the lifetime of the enzyme-substrate complex, the rate of substrate-enzyme binding, and the probability of successful product formation, can all be inferred using these high-order Michaelis-Menten equations. We test our inference procedure to show that it is robust, producing accurate results with only several thousand turnover events per substrate concentration.

Enzymes are biocatalysts that enable numerous reactions in living organisms. The Michaelis-Menten mechanism describes their underlying dynamics[1]. A free enzyme reversibly binds a substrate molecule to form an enzyme-substrate complex that can either lead to the formation of a product via an irreversible catalytic pathway or can simply revert back to the free state without forming a product. Based on this mechanism, the Michaelis-Menten equation predicts a linear relation between the reciprocals of the turnover rate and the substrate concentration. From this linear relation, one can deduce two important kinetic parameters: the maximal rate of the enzymatic reaction and the Michaelis-Menten constant, i.e., the substrate concentration at which half the maximal rate is achieved[2].

Significant technological advancements accomplished in the past two decades have now made it possible to follow the stochastic motion and activity of single particles and molecules[3–11], including individual enzymes[12–19]. Specifically, under certain assumptions, the Michaelis-Menten equation was shown to hold at the single-molecule level where it predicts a linear relation between the mean turnover time and the reciprocal of the substrate concentration[20–25]. The turnover time

[1]School of Chemistry, The Center for Physics and Chemistry of Living Systems, The Raymond and Beverly Sackler Center for Computational Molecular and Materials Science, and The Mark Ratner Institute for Single Molecule Chemistry, Tel Aviv University, 6997801 Tel Aviv, Israel. [2]Department of Environmental Health Sciences, Mailman School of Public Health, Columbia University, New York, NY 10032, USA. e-mail: shlomire@tauex.tau.ac.il

probability distribution can also be measured by tracking single enzymes[12,13,21]. Yet, in contrast to the mean reaction time, higher moments often exhibit complex non-monotonic dependencies on the reciprocal of the substrate concentration[20,21,26,27], which complicates the extraction of kinetic information and the physical interpretation of experimental results.

Some progress can still be made for enzymes whose kinetics are well described by nearest-neighbor models[27]. Expressions for the mean reaction time and the inverse of the squared coefficient of variation have been attained for such enzymes by adopting a Markovian kinetic description in which internal states are linearly connected in a reversible manner[28–30]. Using these, information on the number of interim states involved in substrate binding, the total number of states present in the catalytic network, and the number of non-substrate binding states, can be extracted by measuring the mean and second moment of the catalysis time distribution as a function of substrate concentration[27,29,31,32]. Yet, if the conformational dynamics is non-Markovian[14,33–35], or has parallel branching pathways or non-sequential motifs, this modeling approach fails[27]. One is then left to wonder how to systematically extract useful information from higher moments of enzymatic turnover times in a general way and without making restricting assumptions on the underlying kinetics.

Addressing this research problem, several studies have made distinctive progress within the renewal approach to Michaelis-Menten enzyme kinetics[36–40]. In this approach, one adopts the classical reaction scheme of Michaelis & Menten, but allows for non-Markovian transitions between three coarse-grained enzymatic states: free enzyme and substrate ($E+S$), enzyme-substrate complex (ES), free enzyme and product ($E+P$).

The coarse-grained description effectively accounts for multiple intermediate kinetic states that are often part of the reaction, even when information about them is partially or completely missing due to experimental limitations. It can be built by retaining the same state space as in the classical Michaelis-Menten model, while replacing the familiar transition rates with generally distributed (non-Markovian) transition times[41]. Thus, by allowing for arbitrary transition time distributions, one can effectively account for hidden degrees of freedom, e.g., different conformational states and branching pathways, that are lost in the coarse-graining procedure.

A key insight coming from the renewal approach is that the Michaelis-Menten equation is universal[38]. Namely, regardless of the details of the underlying distributions of binding, unbinding, and catalysis times, the mean turnover time always shows a linear dependence on the reciprocal of the substrate concentration. Yet, extensions of this fundamental result to higher moments of the turnover time have so far remained elusive.

Generalizing the Michaelis-Menten equation to moments of any order will open the door to systematic analysis of turnover time data, thus allowing for characterization of enzyme catalysis beyond the classical, yet incomplete, description of the maximal turnover rate and the Michaelis-Menten constant. Here, we do so by leveraging the renewal approach to identify unique moment combinations that exhibit universal linear dependencies on the reciprocal of the substrate concentration. We call these relations: high-order Michaelis-Menten equations and demonstrate how they can be used to extract kinetic information previously deemed inaccessible, e.g., the binding rate, the mean and variance of the time spent in the bound enzymatic state, and the probability that catalysis occurs before substrate unbinding.

Below, we advance on the renewal framework to derive results for the turnover time distribution and continue to show how these yield high-order Michaelis-Menten equations. The benefits coming from these equations, and how to apply them in practice to infer hidden kinetic parameters, are also discussed in detail.

Results

Renewal approach to enzyme catalysis

Any enzymatic reaction includes three kinetic processes: binding and unbinding of a substrate molecule to and from the enzyme, and catalysis which leads to product formation. These events can be characterized by the random times of binding, T_{on}, unbinding, T_{off}, and of catalysis, T_{cat} (Fig. 1a). Note that at this point we make no assumptions on the distributions of these times, which in turn determine the experimentally observable turnover time: the time it takes a single enzyme to produce a single molecule of product.

The turnover time can be calculated considering two possible routes of enzyme-substrate complex breakup:

$$T_{turn} = T_{on} + \begin{cases} T_{cat} & \text{if } T_{cat} < T_{off} \\ T_{off} + T'_{turn} & \text{if } T_{cat} > T_{off} \end{cases}, \tag{1}$$

where T'_{turn} is an identical and independent copy of T_{turn}. Namely, if T_{cat} is smaller than T_{off}: catalysis follows binding and the enzyme-substrate complex breaks into a free enzyme and product, thus completing the turnover cycle (top row of Eq. (1)). Conversely, if $T_{cat} > T_{off}$: substrate binding is followed by unbinding and the enzyme-substrate complex breaks into a free enzyme and substrate (bottom row of Eq. (1)). In this case, the turnover cycle starts anew.

To move forward, it is convenient to introduce conditional random variables W_{ES}^{cat} and W_{ES}^{off} that stand for the waiting times in the enzyme-substrate complex, provided that either catalysis or unbinding occurs first, respectively. If catalysis occurs first, the waiting time in the enzyme-substrate complex is given by:

$$W_{ES}^{cat} = T_{cat} \,|\, T_{cat} < T_{off}\,, \tag{2}$$

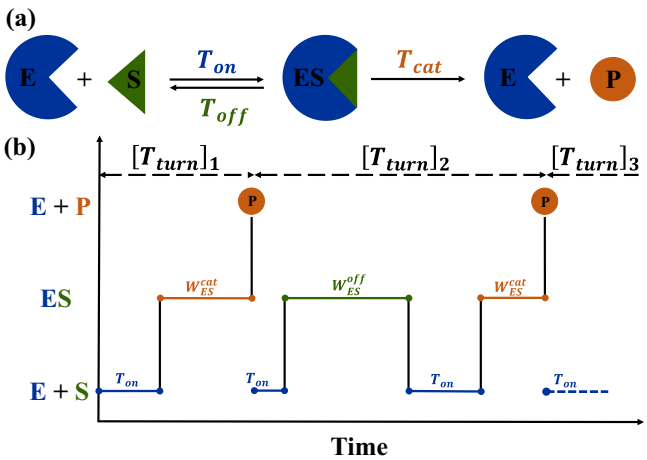

Fig. 1 | Renewal approach to enzyme catalysis. a A schematic representation of the Michaelis-Menten model, where transitions are characterized in terms of a general binding time T_{on}, unbinding time T_{off}, and catalysis time T_{cat}. The free enzyme, E, binds with a substrate molecule, S, to form a bound-enzymatic state, ES. The formed enzyme-substrate complex undergoes catalysis to form a product, P; or goes back to the free enzyme state via unbinding. **b** Turnover time traces representing two consecutive product formation events. Following binding, the enzyme is in the ES state. If catalysis happens prior to unbinding, a product is formed. In this case, the waiting time in the ES state has the statistics of W_{ES}^{cat} from Eq. (2), i.e., of the catalysis time T_{cat} given that it was smaller than the unbinding time T_{off}. Else, unbinding occurs and the waiting time in the ES state has the statistics of W_{ES}^{off} from Eq. (3), i.e., of the unbinding time T_{off} given that it was smaller than the catalysis time T_{cat}. In this paper, we show how to extract hidden information on the statistics of the hidden times T_{on}, W_{ES}^{cat}, W_{ES}^{off} by analyzing the distribution of the turnover time T_{turn} that is observed in experiments.

https://doi.org/10.1038/s41467-025-57327-2

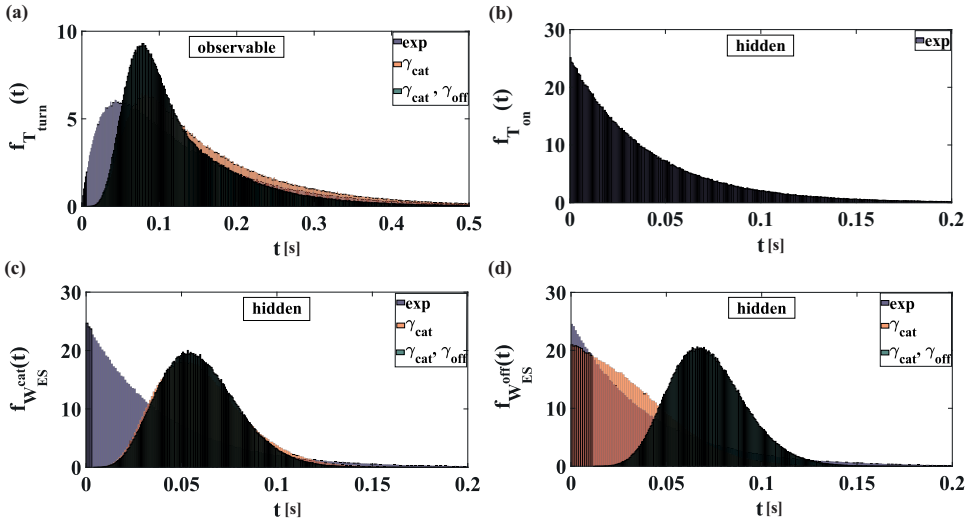

Fig. 2 | Statistics of times characteristic of enzyme kinetics. Several examples of probability distribution functions (PDFs) of **a** the observable turnover times, $f_{T_{turn}}(t)$ and the hidden (**b**) binding times, $f_{T_{on}}(t)$, **c** the conditional catalysis times, $f_{W_{ES}^{cat}}(t)$, and **d** the conditional unbinding times, $f_{W_{ES}^{off}}(t)$. Histograms were obtained from Monte-Carlo simulations of 10^6 turnover cycles of three different illustrative models: (i) the classical single-molecule Michaelis-Menten model, where all kinetic processes are characterized by exponential PDFs (exp: blue bars); (ii) a non-Markovian kinetic scheme, where binding and unbinding times are exponentially distributed but catalysis times follow Gamma-distributions (γ_{cat} : orange bars), and (iii) a non-Markovian scheme where binding times are exponentially distributed but unbinding and catalysis times follow a Gamma-distribution (γ_{cat}, γ_{off}: green bars). Details of the kinetic parameters and probability distribution functions used are provided in the "Methods" section. Codes employed for generating these PDFs have been supplied as Supplementary Software.

and if unbinding occurs first, the waiting time in the enzyme-substrate complex is given by:

$$W_{ES}^{off} = T_{off} \left| T_{cat} > T_{off} \right. . \tag{3}$$

The waiting times in Eqs. (2) and (3) have a clear physical meaning, which allows for an insightful interpretation of the underlying turnover kinetics. In Fig. 1b, we give two possible turnover paths for example. In the first path, binding is directly followed by catalysis and product formation. In the second path, binding is followed by unbinding which restarts the turnover cycle. This is followed by a second binding event leading to catalysis and product formation.

We note that single-molecule experiments are designed to track product formation events, but in most cases cannot follow state changes within the catalytic trajectory. Thus, the statistics of T_{on}, W_{ES}^{cat}, W_{ES}^{off} is hidden and the challenge is to infer them from the observed statistics of the turnover times. Figure 2 illustrates this concept showing the waiting time histograms associated with the probability density functions (PDFs) of the observable turnover time T_{turn} and the hidden times T_{on}, W_{ES}^{cat} and W_{ES}^{off}. Three different examples are considered: (1) a classical single-molecule Michaelis-Menten model, where all kinetic processes are Markovian (characterized by exponential PDFs, blue bars); and (2) two non-Markovian kinetic schemes, where binding times are exponentially distributed but catalysis times follow a Gamma-distribution. The non-Markovian schemes considered differ in the distribution of unbinding times, which is assumed to be exponential in one of them (orange bars) and Gamma-distributed in the other (green bars). Our main goal is to develop an approach for extracting information about the hidden PDFs from single-molecule measurements of the turnover time. Next, we develop the theory and practical tools that allow us to do just that.

The probability density functions of the conditional random variables W_{ES}^{cat} and W_{ES}^{off} can be written in terms of probability density functions of the catalysis and unbinding times, $f_{T_{cat}}(t)$ and $f_{T_{off}}(t)$, as:

$$f_{W_{ES}^{cat}}(t) = \frac{\Pr\left[T_{cat} = t \left| T_{cat} < T_{off}\right.\right]}{\Pr\left[T_{cat} < T_{off}\right]} = \frac{f_{T_{cat}}(t)\bar{F}_{T_{off}}(t)}{\phi_{cat}}, \tag{4}$$

and:

$$f_{W_{ES}^{off}}(t) = \frac{\Pr\left[T_{off} = t \left| T_{cat} > T_{off}\right.\right]}{\Pr\left[T_{cat} > T_{off}\right]} = \frac{f_{T_{off}}(t)\bar{F}_{T_{cat}}(t)}{\phi_{off}}. \tag{5}$$

Here $\bar{F}_{T_{cat}}(t) = \Pr\left[T_{cat} > t\right]$ and $\bar{F}_{T_{off}}(t) = \Pr\left[T_{off} > t\right]$ are the survival probability functions of the catalysis and unbinding times respectively, and $\phi_{cat} = \int_0^\infty f_{T_{cat}}(t)\bar{F}_{T_{off}}(t)dt$ and $\phi_{off} = 1 - \phi_{cat}$ are respectively the probabilities for catalysis to occur before unbinding and vice versa. Naturally, the sum of the probabilities characterizing the splitting of the catalytic and unbinding pathways is equal to unity. The probability density of the unconditional waiting time at the ES state, W_{ES}, is thus given by:

$$f_{W_{ES}}(t) = \phi_{cat} f_{W_{ES}^{cat}}(t) + \left(1 - \phi_{cat}\right) f_{W_{ES}^{off}}(t). \tag{6}$$

Using the above definitions and assuming that binding times are exponentially distributed with a rate $k_{on}[S]$, the Laplace transform of the turnover time, T_{turn} in Eq. (1), can be written as (Supplementary Discussion 2):

$$\hat{f}_{T_{turn}}(k) = \int_0^\infty e^{-kt} f_{T_{turn}}(t)dt = \frac{\phi_{cat}\hat{f}_{W_{ES}^{cat}}(k)}{1 + \frac{k}{k_{on}[S]} + \phi_{cat}\hat{f}_{W_{ES}^{cat}}(k) - \hat{f}_{W_{ES}}(k)}. \tag{7}$$

Equation (7) expresses the statistics of turnover times in terms of physically meaningful quantities: the substrate concentration $[S]$, the binding rate k_{on}, the Laplace transforms $\hat{f}_{W_{ES}^{cat}}(k)$ and $\hat{f}_{W_{ES}}(k)$ of the conditional and unconditional waiting times in the ES state, and the splitting probability ϕ_{cat}. Next, we show how moments of the turnover

time can be used to infer k_{on}, ϕ_{cat}, and moments of the unknown waiting times W_{ES}^{cat} and W_{ES}.

The mean turnover time

The mean turnover time can be computed directly from Eq. (7). It is given by:

$$\langle T_{turn}\rangle = -\left.\frac{\partial \hat{f}_{T_{turn}}(k)}{\partial k}\right|_{k=0} = \overbrace{\left(\frac{1}{\phi_{cat}\,k_{on}}\right)}^{A_1}\frac{1}{[S]} + \overbrace{\frac{\langle W_{ES}\rangle}{\phi_{cat}}}^{B_1}, \tag{8}$$

where $\langle W_{ES}\rangle$ is the mean waiting time in the ES state, and all other parameters were previously defined. Note that Eq. (8) gives a linear relation between the mean turnover time and the reciprocal of the substrate concentration. To this end, we define $A_1 = 1/(\phi_{cat}\,k_{on})$ and $B_1 = \langle W_{ES}\rangle/\phi_{cat}$ as the slope and intercept of the corresponding line, respectively.

When binding, unbinding, and catalysis times are all exponentially distributed with rates k_{on}, k_{off} and k_{cat}, respectively: the mean turnover time in Eq. (8) reduces to the known Michaelis-Menten formula $\langle T_{turn}\rangle = \frac{K_M}{v_{\max}}\frac{1}{[S]} + \frac{1}{v_{\max}}$. Note that in contrast to bulk measurements where $v_{\max} = k_{cat}[E_0]$ with $[E_0]$ standing for the total enzyme concentration, at the single enzyme level we have $v_{\max} = k_{cat}$ for the maximal reaction rate. Also, $K_M = (k_{cat} + k_{off})/k_{on}$ is the Michaelis-Menten constant, which corresponds to the substrate concentration at which half the maximal reaction rate, $v_{\max}$, is achieved.

In Fig. 3a, we plot $\langle T_{turn}\rangle$ vs. the reciprocal of the substrate concentration for the Markovian case described above (blue solid line). Along with this classical case, we have also chosen two other enzymatic systems where kinetic processes are non-Markovian. The orange solid line in Fig. 3a represents the case where T_{cat} follows a Gamma distribution. Similarly, the green solid line represents the case where both T_{cat} and T_{off} follow Gamma distributions (see "Methods" section for details). The corresponding symbols represent simulation data points, which are in accord with theory (solid lines). These results illustrate that the microscopic details of the kinetic transitions do not change the linear dependence on the reciprocal of the substrate concentration as predicted by Eq. (8).

Summarizing, Eq. (8) extends the basic Michaelis-Menten formula to situations where catalysis and unbinding times come from general distributions. We then have $v_{\max} = 1/B_1 = \phi_{cat}/\langle W_{ES}\rangle$ and $K_M = A_1/B_1 = 1/(k_{on}\langle W_{ES}\rangle)$. We thus see that the maximal turnover rate is determined by the ratio of the probability, ϕ_{cat}, for a catalytic event to occur before unbinding and the mean waiting time, $\langle W_{ES}\rangle$, in the ES state. Similarly, the Michaelis-Menten constant is determined by the reciprocal of the product between the binding rate and $\langle W_{ES}\rangle$.

Michaelis-Menten equations for high turnover time moments

As shown in the previous section, the linear relation between the mean turnover time and the reciprocal of the substrate concentration (also known as the Lineweaver–Burk plot) allows us to obtain valuable information on enzymatic activity. This is done by fitting a straight line to the data, extracting the slope A_1, and intercept B_1, of Eq. (8); and determining $v_{\max} = 1/B_1$ and $K_M = A_1/B_1$. However, essential microscopic characteristics, such as k_{on}, ϕ_{cat}, $\langle W_{ES}^{cat}\rangle$, and $\langle W_{ES}\rangle$ still remain unknown.

Higher moments of the turnover time distribution can also be analyzed to try and extract kinetic information. Yet, to date, there was no way of doing so in a manner similar to that in which kinetic information is extracted from the Michaelis-Menten equation. Indeed, one thing that quickly becomes clear is that higher moments display nonlinear dependencies on $1/[S]$. These are illustrated in Fig. 3b, c for the second and third moments of the turnover time, calculated for the different kinetic models that were considered in Fig. 2. Complicated non-linear behaviors are also displayed by other statistical measures of enzymatic activity such as the randomness parameter, Poisson indicator and the Fano factor[20,26,27,30,42]. As an example, we present in Fig. 3d the squared coefficient of variation (randomness parameter), $CV^2 = \frac{\langle T_{turn}^2\rangle - \langle T_{turn}\rangle^2}{\langle T_{turn}\rangle^2}$, which indeed shows a

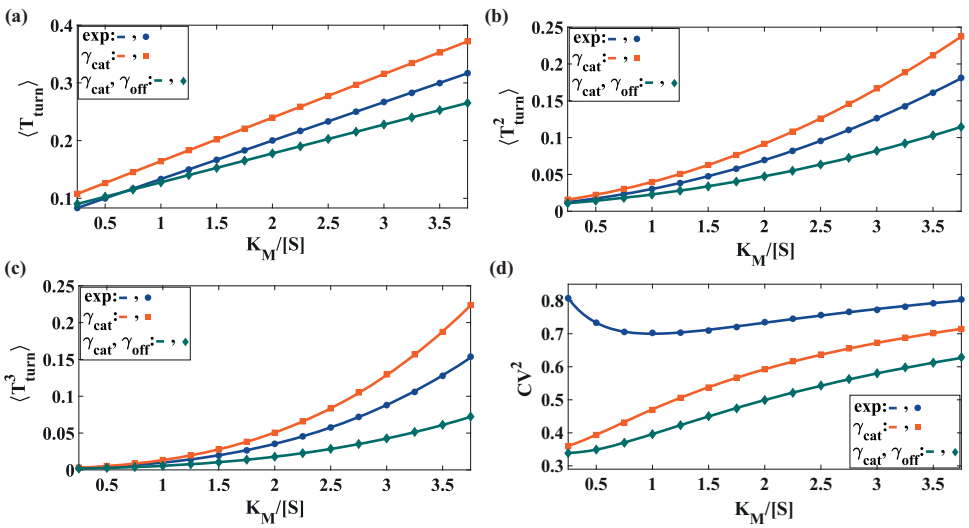

Fig. 3 | Moments and squared coefficient of variation of the turnover time distribution. a The mean turnover time, $\langle T_{turn}\rangle$, as a function of the reciprocal of the substrate concentration, $[S]$ (measured in units of the Michaelis-Menten constant, K_M). We assume a Markovian substrate binding process and consider three different cases for catalysis and unbinding: (i) exponential catalysis and unbinding times (exp : blue), (ii) Gamma distributed catalysis time and exponential unbinding time (γ_{cat} : orange), and (iii) Gamma distributed catalysis and unbinding times (γ_{cat}, γ_{off} : green). Solid lines come from Eq. (8) which is corroborated by numerical simulations (symbols). In all cases the linear relation predicted by Eq. (8) is shown to hold. **b** Same as **a**, but for the second moment $\langle T_{turn}^2\rangle$ of the turnover time. **c** Same as **a**, but for the third moment $\langle T_{turn}^3\rangle$ of the turnover time. **d** Same as **a**, but for the squared coefficient of variation, $CV^2 = \frac{\langle T_{turn}^2\rangle - \langle T_{turn}\rangle^2}{\langle T_{turn}\rangle^2}$. It can be appreciated that higher moments, and the squared coefficient of variation, are highly non-linear with respect to the reciprocal of the substrate concentration. Source data are provided as a Source Data file. Codes employed for generating these data sets have been supplied as Supplementary Software.

https://doi.org/10.1038/s41467-025-57327-2

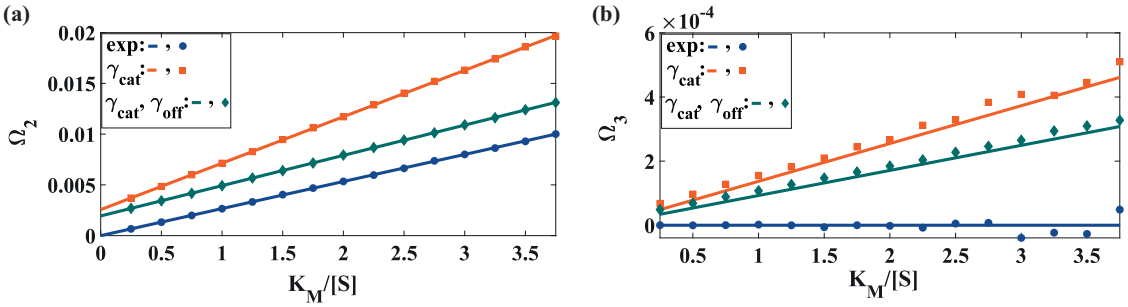

Fig. 4 | High-order Michaelis-Menten equations. a Second order Michaelis-Menten equation. The moments combination, $\Omega_2 = \langle T_{turn} \rangle^2 - \frac{\langle T_{turn}^2 \rangle}{2}$, as a function of the reciprocal of the substrate concentration, $[S]$ (measured in units of the Michaelis constant, K_M). Solid lines come from Eq. (11) which is corroborated by numerical simulations (symbols). In all cases the linear relation predicted by Eq. (11) is shown to hold. **b** Third order Michaelis-Menten equation. The moments combination, $\Omega_3 = \frac{\langle T_{turn}^3 \rangle}{6} - \langle T_{turn} \rangle \langle T_{turn}^2 \rangle + \langle T_{turn} \rangle^3$, as a function of the reciprocal of the substrate concentration (measured in units of the Michaelis constant). Solid lines come from Eq. (12) which is corroborated by numerical simulations (symbols). In all cases the linear relation predicted by Eq. (12) is shown to hold. For both (**a**) and (**b**), we assume a Markovian substrate binding process and consider three different cases for catalysis and unbinding: (i) exponential catalysis and unbinding times (exp : blue), (ii) Gamma distributed catalysis time and exponential unbinding time (γ_{cat} : orange), and (iii) Gamma distributed catalysis and unbinding times (γ_{cat}, γ_{off} : green) [see "Methods" section for details]. Source data are provided as a Source Data file. Codes employed for generating these data sets have been supplied as Supplementary Software.

nonlinear behavior for all considered model systems. Notably, even for the classical Michaelis-Menten model, which is characterized by exponential distributions of binding, unbinding and catalytic times, the randomness parameter exhibits a nonmonotonic dependence on $1/[S]$ (blue line and symbols in Fig. 3d).

Next, we build on Eq. (7) to reveal distinguished combinations of higher-order moments that depend linearly on the reciprocal of the substrate concentration. We show that these newly discovered relations open the door for large-scale characterization of hidden parameters in enzyme kinetics. We start by taking the reciprocal of Eq. (7) to arrive at the following relation:

$$\frac{1}{\hat{f}_{T_{turn}}(k)} = \left(\frac{k}{\phi_{cat} \hat{f}_{W_{ES}^{cat}}(k) k_{on}} \right) \frac{1}{[S]} + \frac{1 - \hat{f}_{W_{ES}}(k)}{\phi_{cat} \hat{f}_{W_{ES}^{cat}}(k)} + 1. \tag{9}$$

Analogous to the Michaelis-Menten equation reported in Eq. (8), the above equation also shows a linear dependence of $1/\hat{f}_{T_{turn}}(k)$ on the reciprocal of the substrate concentration. Expanding both sides of Eq. (9) in a Taylor series with respect to the Laplace variable k, and equating equal order terms, we get (Supplementary Discussion 3):

$$\Omega_n = \frac{A_n}{[S]} + B_n + \delta_{n,0}, \tag{10}$$

where

$$\Omega_n = \frac{\partial^n}{\partial k^n} \left(\frac{1}{\hat{f}_{T_{turn}}(k)} \right) \Big|_{k=0} \frac{1}{n!},$$

and

$$A_n = \left(\frac{1}{\phi_{cat} k_{on}} \right) \frac{\partial^n}{\partial k^n} \left(\frac{k}{\hat{f}_{W_{ES}^{cat}}(k)} \right) \Big|_{k=0} \frac{1}{n!},$$

$$B_n = \left(\frac{1}{\phi_{cat}} \right) \frac{\partial^n}{\partial k^n} \left(\frac{1 - \hat{f}_{W_{ES}}(k)}{\hat{f}_{W_{ES}^{cat}}(k)} \right) \Big|_{k=0} \frac{1}{n!},$$

and where $\delta_{n,0}$ is the Kronecker delta.

For $n = 0$ both the left-hand side and right-hand side of Eq. (10) are equal to unity, indicating that all PDFs composing this equation are properly normalized. Also, for $n = 1$, Eq. (10) reduces to Eq. (8) for the first moment. For $n > 1$ the left-hand side of Eq. (10) is a combination of turnover time moments of order $\{1, \ldots, n\}$ whereas its right-hand side is written in terms of kinetic parameters of the enzymatic process (see Table 1 for $n = 1$, 2, and 3 and Supplementary Discussion 4 for further details). Thus, Eq. (10) provides the desired linear relationship between the turnover time moments and microscopic parameters of the enzyme. Using an analog of the Lineweaver–Burk plot, the parameters A_n and B_n can be found as the slope and intercept of Ω_n when plotted vs. $1/[S]$, respectively. Next, we present and discuss these linear relations for the most important cases of $n = 2$ and 3, which include combinations of second and third-order moments. We then proceed to demonstrate how these relations can be used to infer key parameters of enzymatic catalysis in practice.

Second and third-order Michaelis-Menten equations

Considering second-order terms in Eq. (10), we get the following equation:

$$\Omega_2 = \overbrace{\left(\frac{\langle W_{ES}^{cat} \rangle}{\phi_{cat} k_{on}} \right)}^{A_2} \frac{1}{[S]} + \frac{\overbrace{2\langle W_{ES}^{cat} \rangle \langle W_{ES} \rangle - \langle W_{ES}^2 \rangle}^{B_2}}{2\phi_{cat}}, \tag{11}$$

where $\Omega_2 = \langle T_{turn} \rangle^2 - \frac{\langle T_{turn}^2 \rangle}{2}$ is the specific combination of $n \le 2$ turnover time moments, which shows a linear dependence on $1/[S]$ (see Fig. 4a). For the classical Michaelis-Menten model, characterized by exponential time distributions, the various PDFs that determine the form of Eq. (10), $f_{W_{ES}^{cat}}(t)$, $f_{W_{ES}^{off}}(t)$ and $f_{W_{ES}}(t)$, have exactly the same functional form: $(k_{cat} + k_{off}) e^{-(k_{cat} + k_{off})t}$ (Supplementary Discussion 5). Thus, in this case $\langle W_{ES} \rangle = \langle W_{ES}^{cat} \rangle$ and we have $2\langle W_{ES}^{cat} \rangle \langle W_{ES} \rangle - \langle W_{ES}^2 \rangle = 2\langle W_{ES} \rangle^2 - \langle W_{ES}^2 \rangle = 0$, where the last equality follows from basic properties of the exponential distribution. The parameter B_2 which gives the intersection of the line Ω_2 with the vertical axis, is then equal to zero (blue line in Fig. 4a). However, this is not true in general. For non-exponential distributions of catalytic and unbinding times, B_2 can be nonzero (orange and green lines in Fig. 4a). Thus, a non-zero value of B_2 can serve as an indicator of the non-classical nature of the enzyme being studied.

Table 1 | Explicit expressions for Ω_n, A_n, B_n from Eq. (10), for $n = 1, 2, 3$

n	Ω_n	A_n	B_n
1	$\langle T_{turn}\rangle$	$\frac{1}{\phi_{cat}k_{on}}$	$\frac{\langle W_{ES}\rangle}{\phi_{cat}}$
2	$\langle T_{turn}\rangle^2 - \frac{\langle T_{turn}^2\rangle}{2}$	$\frac{\langle W_{ES}^{cat}\rangle}{\phi_{cat}k_{on}}$	$\frac{2\langle W_{ES}^{cat}\rangle\langle W_{ES}\rangle - \langle W_{ES}^2\rangle}{2\phi_{cat}}$
3	$\frac{\langle T_{turn}^3\rangle}{6} - \langle T_{turn}\rangle\langle T_{turn}^2\rangle + \langle T_{turn}\rangle^3$	$\frac{\left(\langle W_{ES}^{cat}\rangle^2 - \frac{\langle (W_{ES}^{cat})^2\rangle}{2}\right)}{\phi_{cat}k_{on}}$	$\frac{\left(\frac{\langle W_{ES}^3\rangle}{6} - \frac{\langle W_{ES}^{cat}\rangle\langle W_{ES}^2\rangle}{2} + \langle W_{ES}\rangle\langle W_{ES}^{cat}\rangle^2 - \frac{\langle W_{ES}\rangle\langle (W_{ES}^{cat})^2\rangle}{2}\right)}{\phi_{cat}}$

Note that Ω_n is written in terms of measurable turnover time moments of order $\le n$, and the parameters A_n and B_n, can be determined as the slope and intercept of Ω_n when it is plotted vs. $1/[S]$, respectively. After they are determined, A_n and B_n provide two equations for the unknown kinetics parameters for every moment order n that is analyzed. Here $\langle T_{turn}^n\rangle$ is the nth moment of the turnover time distribution, ϕ_{cat} is the splitting probability of catalysis, k_{on} is the binding rate, $\langle W_{ES}^n\rangle$ is the nth moment of the waiting time in the bound enzymatic state, and $\left\langle (W_{ES}^{cat})^n\right\rangle$ is the nth moment of the waiting time in the bound enzymatic state conditioned on catalysis occurring prior to unbinding.

Considering third-order terms in Eq. (10) we get the following equation:

$$\Omega_3 = \overbrace{\left(\frac{\langle W_{ES}^{cat}\rangle^2 - \frac{\langle (W_{ES}^{cat})^2\rangle}{2}}{\phi_{cat}k_{on}}\right)}^{A_3}\frac{1}{[S]} + \overbrace{\frac{\left(\frac{\langle W_{ES}^3\rangle}{6} - \frac{\langle W_{ES}^{cat}\rangle\langle W_{ES}^2\rangle}{2} + \langle W_{ES}\rangle\langle W_{ES}^{cat}\rangle^2 - \frac{\langle W_{ES}\rangle\langle (W_{ES}^{cat})^2\rangle}{2}\right)}{\phi_{cat}}}^{B_3}, \quad (12)$$

where $\Omega_3 = \frac{\langle T_{turn}^3\rangle}{6} - \langle T_{turn}\rangle\langle T_{turn}^2\rangle + \langle T_{turn}\rangle^3$ is the specific combination of $n \le 3$ turnover time moments, which shows a linear dependence on $1/[S]$ (see Fig. 4b). Here too, we see a clear difference between the classical Michaelis-Menten model which is characterized by exponential time distributions, and non-Markovian scenarios. Specifically, in the Markovian case we find that $A_3 = B_3 = 0$ (Supplementary Discussion 6), i.e., the slope and the intercept in Eq. (12) vanish (blue line in Fig. 4b). Once again, note that this is not true in general. For non-exponential distributions of catalysis and unbinding times, A_3 and B_3 can be nonzero (orange and green lines in Fig. 4b).

Inferring hidden kinetic parameters from high-order Michaelis-Menten equations

Considering Eqs. (8) and (11) for Ω_1 and Ω_2, respectively, we observe that they include four measurable quantities, A_1, B_1, A_2, B_2, and five unknown kinetic parameters, ϕ_{cat}, k_{on}, $\langle W_{ES}\rangle$, $\langle W_{ES}^{cat}\rangle$, $\langle W_{ES}^2\rangle$, that characterize enzymatic activity (see Table 1). Since an additional equation is missing, these kinetic parameters cannot be uniquely determined only by analyzing the dependence of Ω_1 and Ω_2 on the reciprocal of the substrate concentration. This problem cannot be resolved by considering combinations of higher turnover time moments, Ω_n, with $n > 2$. Indeed, for any M, the set of Ω_n, with $n \le M$ allows to obtain $2M$ quantities, A_n and B_n, the values of which are determined by $2M+1$ unknown kinetic parameters. In particular, plotting Ω_1, Ω_2 and Ω_3 vs. $1/[S]$ one can find six quantities, A_n and B_n for $n \le 3$, which are expressed in terms of seven unknown kinetic parameters, ϕ_{cat}, k_{on}, $\langle W_{ES}\rangle$, $\langle W_{ES}^{cat}\rangle$, $\langle W_{ES}^2\rangle$, $\langle (W_{ES}^{cat})^2\rangle$ and $\langle W_{ES}^3\rangle$ (see Table 1).

From here, one can proceed in multiple ways. First, observe that even if just one of the unknown kinetic parameters can be measured independently, this will provide a closure relation for the set of equations and allow for unique determination of all the other unknown parameters. However, this entails direct measurements of e.g., the splitting probability ϕ_{cat} or the mean time spent in the ES state, i.e., $\langle W_{ES}\rangle$. While such direct measurements may be hard to perform, it is noteworthy that when they are feasible, they can be synergistically combined with the framework developed herein to infer hidden kinetic parameters.

Interestingly, missing information can also come from carefully examining other features of the turnover time distribution. In this paper, we focused on moments of the turnover time, but it has recently been shown that short-time behavior also holds valuable kinetic information[43–45]. Specifically, we have recently shown that the short time behavior of the enzymatic turnover time holds information that allows one to uniquely determine the binding rate k_{on}, provided some mild assumptions hold[46]. Plugging in the value of the inferred binding rate into the higher-order Michaelis-Menten equations we have developed herein, provides the required closure and allows one to uniquely determine the values of all the other kinetic parameters.

Finally, we show that one can proceed even in the absence of additional information to obtain approximate estimates of the unknown kinetic parameters. In what follows, we show that these approximations are exact for Markovian enzymes, and then proceed to investigate the role of non-Markovianity. For this purpose, using Table 1, it is useful to present the desired quantities, such as the binding rate k_{on}, and the conditional probability for catalysis to happen before unbinding ϕ_{cat}, in the following form:

$$k_{on} = \left(\frac{B_1}{A_2}\right)\left(\frac{\langle W_{ES}\rangle}{\langle W_{ES}^{cat}\rangle}\right)^{-1}, \quad (13)$$

and

$$\phi_{cat} = \left(\frac{A_2}{A_1B_1}\right)\left(\frac{\langle W_{ES}\rangle}{\langle W_{ES}^{cat}\rangle}\right). \quad (14)$$

From Table 1, we also see that the mean conditional catalysis time $\langle W_{ES}^{cat}\rangle$ can be calculated using the measured slopes of Ω_1, and Ω_2 vs. $1/[S]$ without any additional assumptions and written as:

$$\langle W_{ES}^{cat}\rangle = \left(\frac{A_2}{A_1}\right). \quad (15)$$

Multiplying both sides of Eq. (15) by $\langle W_{ES}\rangle/\langle W_{ES}^{cat}\rangle$, we can write the mean time in the bound enzymatic state as:

$$\langle W_{ES}\rangle = \left(\frac{A_2}{A_1}\right)\left(\frac{\langle W_{ES}\rangle}{\langle W_{ES}^{cat}\rangle}\right), \quad (16)$$

which has a similar form to Eqs. (13) and (14).

Equations (13), (14), and (16) still do not allow us to determine k_{on}, ϕ_{cat} and $\langle W_{ES}\rangle$, since in addition to the measurable quantities, $\left(\frac{B_1}{A_2}\right)$, $\left(\frac{A_2}{A_1B_1}\right)$ and $\left(\frac{A_2}{A_1}\right)$ they also include the unknown ratio $\frac{\langle W_{ES}\rangle}{\langle W_{ES}^{cat}\rangle}$. Yet, recall that we have just shown that for classically behaving enzymes, where

https://doi.org/10.1038/s41467-025-57327-2

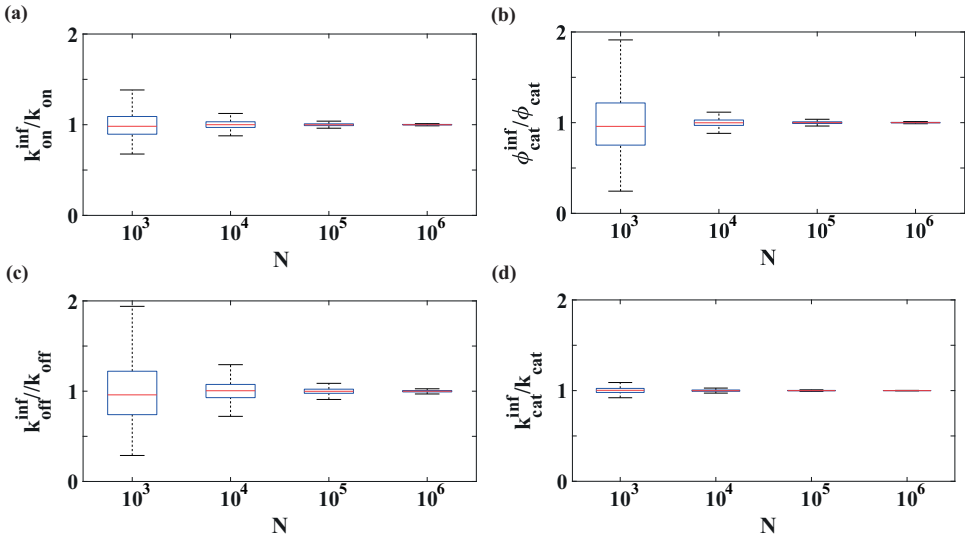

Fig. 5 | Accuracy of the inferred kinetic parameters as a function of the sample size for the Markovian model. Boxplots for the inferred **a** binding rate $\left(k_{on}^{\inf}\right)$, **b** splitting probability of catalysis $\left(\phi_{cat}^{\inf}\right)$, **c** unbinding rate $\left(k_{off}^{\inf}\right)$, and **d** catalysis rate $\left(k_{cat}^{\inf}\right)$ normalized by the corresponding true values $\left(k_{on}, \phi_{cat}, k_{off}, k_{cat}\right)$ and plotted as a function of the number of turnover events, N, per substrate concentration. For each N, 10^3 independent repetitions were performed. The bottom and top of each box are the 25th and 75th percentiles of the sample, respectively, red lines mark the median value, and whiskers extend to 1.5 times the interquartile range. Source data are provided as a Source Data file. Codes employed for generating these data sets have been supplied as Supplementary Software.

all the kinetic processes are Markovian, we have $\frac{\langle W_{ES}\rangle}{\langle W_{ES}^{cat}\rangle}=1$. In this case, k_{on} and ϕ_{cat} can be directly determined from the slopes (A_1, and A_2) and intercept (B_1) of the Ω_1 and Ω_2 lines, as follows:

$$k_{on}=\left(\frac{B_1}{A_2}\right),\ \phi_{cat}=\left(\frac{A_2}{A_1B_1}\right). \tag{17}$$

In addition, the rates of unbinding and catalysis can also be inferred from the slopes (A_1, and A_2) and intercept (B_1) as:

$$k_{off}=\frac{A_1}{A_2}-\frac{1}{B_1},\ \text{and}\ k_{cat}=\frac{1}{B_1}. \tag{18}$$

It should be noted that traditional analysis of enzymatic kinetics, which is based only on measurements of the mean turnover times, cannot provide this important information.

Equations (17) and (18) instruct us on how to infer all the characteristic rates, and the fertility fraction (splitting probability) of catalysis, for Markovian enzymes. However, single molecule measurements are intrinsically stochastic and therefore the accuracy of the inferred kinetic parameters depends on the amount of available data. To address this important issue, we present in Fig. 5 boxplots, characterizing spread and skewness of the inferred kinetic parameters as a function of the number of turnover events per substrate concentration, N. Data were obtained by simulating the classical Michaelis-Menten model with the same parameters as in Fig. 3a (blue line and symbols, see also "Methods" section).

The inference procedure was implemented as follows. The quantities Ω_1 and Ω_2 were estimated based on their relation to the turnover time moments (First column of Table 1). The results were plotted as a function of the reciprocal of the substrate concentration and fitted to obtain estimates for $A_1, B_1, A_2,$ and B_2. Eqs. (17) and (18) were then used to obtain estimates of $k_{on}, \phi_{cat}, k_{off}$ and k_{cat}. To assess the fidelity of this procedure, it was repeated 10^3 times. The presented results show that 10^3 turnover events per substrate concentration were already enough to produce reasonable estimates, and that 10^4 turnover events per substrate concentration gave good estimates. More data leads to an even better accuracy, such that 10^6 turnover events provide near-perfect estimates. We quantify this improving trend in Supplementary Fig. 2, as part of Supplementary Discussion 7. There we show that the normalized standard deviations of our estimates obey the typical $\sim 1/\sqrt{N}$ scaling law.

Kinetic inference for non-Markovian enzymes

For non-Markovian enzymes, one can estimate $k_{on}, \phi_{cat},$ and $\langle W_{ES}\rangle$ by plugging in the closure relation $\frac{\langle W_{ES}\rangle}{\langle W_{ES}^{cat}\rangle}=1$ in Eqs. (13), (14) and (16). Yet, the quality of this approximation depends on whether the unknown ratio does indeed remain relatively close to unity. In other words, any deviation of $\frac{\langle W_{ES}\rangle}{\langle W_{ES}^{cat}\rangle}$ from unity indicates non-Markovian behavior, and the exact value of this ratio provides a measure for the magnitude of the error made when the closure relation is applied. For example, if $\frac{\langle W_{ES}\rangle}{\langle W_{ES}^{cat}\rangle}=2$, applying the closure relation $\frac{\langle W_{ES}\rangle}{\langle W_{ES}^{cat}\rangle}=1$ in Eq. (13) will overestimate the true values of k_{on} by a factor of two, and similar logic carries to the error made when using the closure relation to evaluate ϕ_{cat} and $\langle W_{ES}\rangle$ via Eqs. (14) and (16), respectively.

It is thus important to understand in which cases $\frac{\langle W_{ES}\rangle}{\langle W_{ES}^{cat}\rangle}\approx 1$ provides a fair approximation for non-Markovian enzymes. To answer this question, we now analyze two prevalent, yet distinctly different, types of non-Markovian behavior in enzymes. Namely, non-Markovian behavior that arises due to sequential catalytic steps and non-Markovian behavior that arises due to parallel catalytic pathways. Non-exponential catalysis times are common to both scenarios. Yet, for sequential catalytic steps we have catalysis time distributions that are narrower than the exponential and $\frac{\langle W_{ES}\rangle}{\langle W_{ES}^{cat}\rangle}<1$, whereas for parallel catalytic pathways we have catalysis time distributions that are broader than the exponential and $\frac{\langle W_{ES}\rangle}{\langle W_{ES}^{cat}\rangle}>1$.

Let us first consider a model involving two sequential catalytic steps (Fig. 6a). In this model: (1) a free-enzyme, E, can reversibly bind a substrate S with rate $k_{on}[S]$, to form an enzyme-substrate complex, ES_1; (2) the complex ES_1 can then be irreversibly transformed into another

https://doi.org/10.1038/s41467-025-57327-2

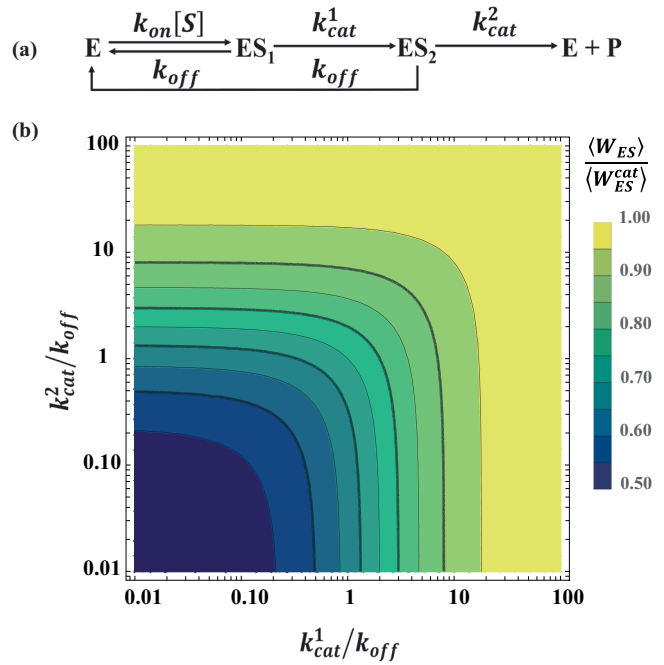

Fig. 6 | Sequential reaction mechanism. a A schematic representation of a model involving two sequential catalytic steps. The free enzyme, E undergoes binding with a substrate to form the first substrate-bound conformer ES_1 that sequentially transitions to the second bound-enzymatic state, ES_2. This state can lead to the formation of the product, P, through an irreversible catalytic event. From the bound states ES_1 and ES_2, unbinding events can occur—leading back to the free enzyme. The described kinetic processes are characterized by the rates of binding $(k_{on}[S])$ where $[S]$ is the substrate concentration, unbinding $\left(k_{off}\right)$, the first catalytic transition $\left(k^1_{cat}\right)$, and the second catalytic transition that forms the product $\left(k^2_{cat}\right)$. **b** 2D color map of the error factor $\frac{\langle W_{ES}\rangle}{\langle W^{cat}_{ES}\rangle}$ in the space of the normalized catalytic rates $\frac{k^1_{cat}}{k_{off}}$ and $\frac{k^2_{cat}}{k_{off}}$. Here $\langle W_{ES}\rangle$ and $\langle W^{cat}_{ES}\rangle$ are the mean waiting times of the bound-enzymatic state and the conditional catalysis times, respectively.

complex, ES_2, with rate k^1_{cat} or, alternatively, unbind with rate k_{off}; and finally (3) the complex ES_2 can be converted by the enzyme to form a product, P, with rate k^2_{cat} or unbind with rate k_{off}. Note that the kinetic scheme in Fig. 6a can be mapped onto the renewal kinetic scheme in Fig. 1a by coarse graining ES_1 and ES_2 into a single ES state and defining T_{off} and T_{cat} accordingly (Supplementary Discussion 8). This fact allows us to use the results derived in the previous sections.

For the sequential scheme in Fig. 6a, the ratio $\frac{\langle W_{ES}\rangle}{\langle W^{cat}_{ES}\rangle}$ can be calculated analytically, and we find it is given by (Supplementary Discussion 9):

$$\frac{\langle W_{ES}\rangle}{\langle W^{cat}_{ES}\rangle}=\frac{k^1_{cat}+k^2_{cat}+k_{off}}{k^1_{cat}+k^2_{cat}+2k_{off}}. \tag{19}$$

Importantly, Eq. (19) asserts that for any choice of kinetic parameters the ratio lies in the range of $1/2\le\frac{\langle W_{ES}\rangle}{\langle W^{cat}_{ES}\rangle}<1$, which provides a tight bound on the error coming from the use of the closure relation. We visually illustrate this in Fig. 6b which presents a 2D color map of $\frac{\langle W_{ES}\rangle}{\langle W^{cat}_{ES}\rangle}$, calculated in the space of the normalized catalytic rates $\frac{k^1_{cat}}{k_{off}}$ and $\frac{k^2_{cat}}{k_{off}}$. It can be seen that the largest deviations from the classical Markovian behavior, $\frac{\langle W_{ES}\rangle}{\langle W^{cat}_{ES}\rangle}=1$, occur when the unbinding rate is much larger than both catalytic rates, $k_{off}\gg k^1_{cat}+k^2_{cat}$.

Summarizing, for enzymes that follow the successive catalytic scheme illustrated in Fig. 6a, the desired kinetic parameters k_{on} and ϕ_{cat} can be well estimated by setting $\frac{\langle W_{ES}\rangle}{\langle W^{cat}_{ES}\rangle}=1$ in Eqs. (13) and (14). Also, the mean waiting time in the coarse grained ES state can be estimated via Eq. (16) since under the above closure relation, $\langle W_{ES}\rangle=\langle W^{cat}_{ES}\rangle$. Using the closure relation $\frac{\langle W_{ES}\rangle}{\langle W^{cat}_{ES}\rangle}=1$, results in an error factor of no more than two. For example, the binding rate is underestimated compared to its true value, but in no more than a factor of two. In Supplementary Discussion 10, we test the sensitivity of our inference procedure to the amount of available data. For the sequential reaction mechanism described above, we reach similar conclusions as those obtained for the Markovian case where all kinetic processes were exponentially distributed (Supplementary Fig. 3).

We also extended the above analysis to kinetic models with n identical sequential steps (Supplementary Discussion 11). We show that the maximal error factor is then given by n. Since for real enzymes the value of n is rather limited, the closure relation $\frac{\langle W_{ES}\rangle}{\langle W^{cat}_{ES}\rangle}=1$ can be applied to sequential enzymes yielding estimates that are well within an order of magnitude to the true parameter values.

Next, we consider a reaction scheme involving two parallel catalytic pathways (Fig. 7a). In this model: (1) a free-enzyme, E, reversibly binds a substrate, S, to form either the enzyme-substrate complex ES_1 or the enzyme-substrate complex ES_2 with rates $pk_{on}[S]$ and $(1-p)k_{on}[S]$, respectively, where p is the splitting probability between pathways; (2) both complexes can then be converted to a product, P, with rates k^1_{cat} or k^2_{cat}, respectively; or unbind with a common rate k_{off}. Unlike the sequential scheme, here the formation of a product can occur from both enzyme-substrate complexes, ES_1 and ES_2. We once again note that the kinetic scheme in Fig. 7a can also be described in the language of Fig. 1a by coarse-graining ES_1 and ES_2 into a single ES state and defining T_{off} and T_{cat} accordingly (Supplementary Discussion 12). This fact allows us to use the results derived in the previous sections.

For the parallel kinetic scheme, the ratio $\frac{\langle W_{ES}\rangle}{\langle W^{cat}_{ES}\rangle}$ can be calculated analytically, and we find it is given by (Supplementary Discussion 13):

$$\frac{\langle W_{ES}\rangle}{\langle W^{cat}_{ES}\rangle}=\frac{\left(k^1_{cat}+k_{off}+p\left(k^2_{cat}-k^1_{cat}\right)\right)\left((1-p)k^2_{cat}k_{off}+k^1_{cat}\left(k^2_{cat}+pk_{off}\right)\right)}{pk^1_{cat}\left(k^2_{cat}+k_{off}\right)^2+(1-p)k^2_{cat}\left(k^1_{cat}+k_{off}\right)^2}. \tag{20}$$

Analysis of this equation asserts that the ratio $\frac{\langle W_{ES}\rangle}{\langle W^{cat}_{ES}\rangle}$ exhibits the strongest deviations from unity for the splitting probability $p=0.5$, i.e., when the two enzyme-substrate complexes are formed with equal probability. We thus focus on this worst-case scenario.

The corresponding 2D color map of $\frac{\langle W_{ES}\rangle}{\langle W^{cat}_{ES}\rangle}$, calculated as a function of the normalized catalytic rates $\frac{k^1_{cat}}{k_{off}}$ and $\frac{k^2_{cat}}{k_{off}}$ is presented in Fig. 7b. This map clearly demonstrates that in most of the parameter space the ratio $\frac{\langle W_{ES}\rangle}{\langle W^{cat}_{ES}\rangle}$ is close to unity, albeit in small corner regions where significant deviations from unity are observed. This happens under extreme conditions where the normalized catalytic rates, $\frac{k^1_{cat}}{k_{off}}$ and $\frac{k^2_{cat}}{k_{off}}$, differ from each other by more than three orders of magnitude; and note that in all other cases applying the closure relation $\frac{\langle W_{ES}\rangle}{\langle W^{cat}_{ES}\rangle}=1$ in Eqs. (13), (14), and (16) will lead to estimates that are withing an order of magnitude from true values. Similar analysis applies to asymmetric cases where one of the catalytic routes is preferentially chosen over the other ($p\neq0.5$), albeit systematic estimation errors being even smaller (Supplementary

https://doi.org/10.1038/s41467-025-57327-2

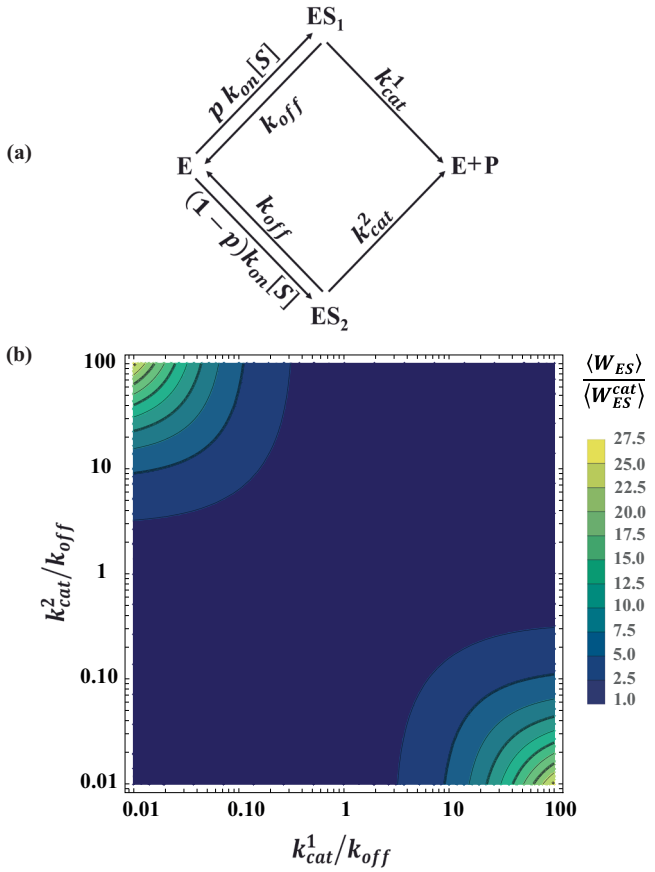

Fig. 7 | Parallel reaction mechanism. a A schematic representation of a model involving two parallel catalytic steps. The free enzyme, E can bind with a substrate molecule via two parallel processes to form the first substrate-bound conformer, ES_1 or the second bound-enzymatic state, ES_2. These branched substrate-binding channels have splitting probabilities p and $1-p$, respectively. Both bound states can form the product, P through irreversible catalytic events. From ES_1 and ES_2, unbinding events can occur that lead back to the free enzyme. The described kinetic processes are characterized by the rates of binding $(k_{on}[S])$ where $[S]$ is the substrate concentration, unbinding $\left(k_{off}\right)$, the first $\left(k^1_{cat}\right)$ and second $\left(k^2_{cat}\right)$ catalytic transitions, respectively. **b** 2D color map of the error factor $\frac{\langle W_{ES}\rangle}{\langle W^{cat}_{ES}\rangle}$ in the space of the normalized catalytic rates $\frac{k^1_{cat}}{k_{off}}$ and $\frac{k^2_{cat}}{k_{off}}$, for the splitting probability $p=0.5$. Here $\langle W_{ES}\rangle$ and $\langle W^{cat}_{ES}\rangle$ are the mean waiting times of the bound-enzymatic state and the conditional catalysis times, respectively. Note that for $\frac{k^1_{cat}}{k_{off}}$ and $\frac{k^2_{cat}}{k_{off}}$ that span four orders of magnitude, the error factor is always <30, and in most cases significantly smaller than this upper bound.

Discussion 14). Thus, similar to the sequential scheme, setting $\frac{\langle W_{ES}\rangle}{\langle W^{cat}_{ES}\rangle}=1$ as a closure relation in the parallel kinetic scheme leads to very good approximations for the values of kinetic parameters that are otherwise very hard to estimate.

Discussion

In this paper, we presented a pioneering approach to enzyme kinetics at the single-molecule level. Building on a renewal approach to enzyme kinetics, we derived a set of high-order Michaelis-Menten equations that reveal universal linear dependencies between unique combinations of turnover time moments and the reciprocal of the substrate concentration. These relations effectively generalize the single-molecule Michaelis-Menten equation from the mean turnover time to moments of arbitrary order.

We demonstrated the capacity of our approach to infer concealed kinetic parameters, such as the lifetime of the enzyme-substrate complex, the rate of binding, and the probability of successful product formation. With this, we pave the way for systematic characterization of enzyme kinetics from single-molecule data, going well beyond the limited information provided by the all-familiar Michaelis-Menten constant and maximal reaction velocity.

The results apply to Markovian and non-Markovian enzymes alike. For Markovian enzymes, which adhere to memoryless stochastic transitions between states, the framework provides a way to accurately estimate kinetic parameters such as the binding, unbinding and catalysis rates. By leveraging the high-order Michaelis-Menten equations, which capture universal linear dependencies, precise determination of these parameters is achieved.

For non-Markovian enzymes, where kinetic processes exhibit memory effects, our framework is also exact but incomplete. Namely, for inference using our framework to be exact, one of the unknown kinetic parameters, e.g., the binding rate, must be measured or inferred independently. This is not a serious limitation as the binding rate can be inferred based on information held in the short-time tail of the turnover time distribution, provided some mild assumptions hold[46]. Combining such additional information with the results derived herein gives a closed and complete inference framework for non-Markovian enzymes.

Moreover, our framework can be used on non-Markovian enzymes even in lieu of external information on the binding rate or other kinetic parameters. To this end, one assumes that the mean time spent in the enzyme-substrate complex is identical to the (conditional) mean time spent in this complex provided product formation is the direct result of the enzyme-substrate encounter. While this approximation introduces some error, we find that this is typically limited. We demonstrated this by analyzing kinetic models with sequential and parallel product formation pathways. These models display canonical, yet completely orthogonal, types of non-Markovian behavior. Nevertheless, in all cases considered, we showed that applying the above assumption provides estimates that are within an order of magnitude from the true value of kinetic parameters that would otherwise remain completely unknown.

In summary, through the derivation of high-order Michaelis-Menten equations, we have shown that traditional analysis methods in enzymology can be extended to unveil central kinetic parameters that have so far remained hidden. We thus offer a systematic and straightforward approach to characterize enzyme kinetics far and beyond the current state of the art.

Methods

Kinetic parameters used in Figs. 2–4

The results presented in Figs. 2–4 were obtained considering three different catalytic models: (1) exponential catalysis and unbinding times (blue), (2) Gamma distributed catalysis times and exponential unbinding times (orange), and (3) Gamma distributed catalysis and unbinding times (green). Data coming from numerical simulations, histograms in Fig. 2 and symbols in Figs. 3 and 4, were obtained by taking 10^6 turnover events at each substrate concentration, for each one of the cases discussed below.

The substrate binding event is common in all three enzymatic systems. It is governed by an exponential distribution with a mean binding time of $\langle T_{on}\rangle=(k_{on}[S])^{-1}\equiv(5^*[S])^{-1}$ [s]. In the first model, exponential catalysis and unbinding times, the mean unbinding and catalysis times were taken to be $\left\langle T_{off}\right\rangle=\left(k_{off}\right)^{-1}=1/10$ [s] and $\langle T_{cat}\rangle=(k_{cat})^{-1}=1/15$ [s], respectively. Thus, following the definition of the Michaelis-Menten constant, we have $K_M=\frac{k_{cat}+k_{off}}{k_{on}}=5$ [μM]. This concentration was also used in Fig. 2 where we have set $[S]=5$ [μM]

throughout. The substrate concentrations used in Figs. 3 and 4 lie in the range: $0.2K_M - 4K_M$, where the reciprocal of the substrate concentrations are regularly spaced to ensure uniform coverage of the horizontal axis. All concentrations were normalized by the Michaelis-Menten constant above, i.e., $K_M = 5\,[\mu M]$.

In the second model, Gamma distributed catalysis times and exponential unbinding times, the unbinding time distribution was taken to be the same as in the first case, and catalysis times were taken to follow a Gamma distribution of the form, $f_{T_{cat}}(t) = \frac{e^{\frac{-t}{\theta}} t^{k-1}}{\theta^k \Gamma[k]}$, with shape factor $k = 6\frac{2}{3}$ and scale factor $\theta = \frac{1}{100}$ [s]. The parameters of the Gamma distribution were chosen such that the mean catalysis time for this system, $\langle T_{cat} \rangle = k\theta = 1/15\,[s]$, would be identical to the mean catalysis time of the exponential case, $\langle T_{cat} \rangle = \frac{1}{k_{cat}} = 1/15\,[s]$, thereby allowing for a fair comparison.

In the third model, both the catalytic and unbinding times follow Gamma distributions. The parameters for the catalytic time distribution are the same as in the second case, while the unbinding time distribution has a form, $f_{T_{off}}(t) = \frac{e^{\frac{-t}{\theta}} t^{k-1}}{\theta^k \Gamma[k]}$, with shape factor $k = 10$ and scale factor $\theta = \frac{1}{100}$ [s]. Note that these kinetic parameters were intentionally chosen such that the mean unbinding time, $\left\langle T_{off} \right\rangle = k\theta = \frac{1}{10}[s]$, is exactly equal to the inverse of the unbinding rate constant used for the exponential case, $\left\langle T_{off} \right\rangle = \frac{1}{k_{off}} = \frac{1}{10}[s]$.

In Supplementary Fig. 1, we give histograms of the catalysis and unbinding times that were used in the three models described above. It can be seen that these underlying distributions are qualitatively different from one another, which emphasizes our main point: the set of high-order Michaelis-Menten equations is valid regardless of the underlying kinetics.

Reporting summary

Further information on research design is available in the Nature Portfolio Reporting Summary linked to this article.

Data availability

The authors declare that the data supporting the findings of this study are available within the paper and its Supplementary Information files. Source data are provided with this paper.

Code availability

All the relevant codes used for generating numerical data were provided at the time of submission as Supplementary Software.

References

1. Michaelis, L. & Menten, M. L. Die kinetik der invertinwirkung. *Biochem. Z.* **49**, 333–369 (1913).
2. Segel, I. H. *Enzyme Kinetics: Behavior and Analysis of Rapid Equilibrium and Steady State Enzyme Systems*, Vol. 115 (Wiley, 1975).
3. Moerner, W. E. & Fromm, D. P. Methods of single-molecule fluorescence spectroscopy and microscopy. *Rev. Sci. Instrum.* **74**, 3597–3619 (2003).
4. Yang, H. et al. Protein conformational dynamics probed by single-molecule electron transfer. *Science* **302**, 262–266 (2003).
5. Kulzer, F. & Orrit, M. SIngle-molecule Optics. *Annu. Rev. Phys. Chem.* **55**, 585–611 (2004).
6. Roy, R., Hohng, S. & Ha, T. A practical guide to single-molecule FRET. *Nat. Methods* **5**, 507–516 (2008).
7. Barkai, E., Garini, Y. & Metzler, R. Strange kinetics of single molecules in living cells. *Phys. Today* **65**, 29–35 (2012).
8. Granik, N. et al. Single-particle diffusion characterization by deep learning. *Biophys. J.* **117**, 185–192 (2019).
9. Rehfeldt, F. & Weiss, M. The random walker's toolbox for analyzing single-particle tracking data. *Soft Matter* **19**, 5206–5222 (2023).
10. Scott, S. et al. Extracting, quantifying, and comparing dynamical and biomechanical properties of living matter through single particle tracking. *Phys. Chem. Chem. Phys.* **25**, 1513–1537 (2023).
11. Schanda, P. & Haran, G. NMR and single-molecule FRET insights into fast protein motions and their relation to function. *Annu. Rev. Biophys.* **53**, 247–273 (2024).
12. Funatsu, T., Harada, Y., Tokunaga, M., Saito, K. & Yanagida, T. Imaging of single fluorescent molecules and individual ATP turnovers by single myosin molecules in aqueous solution. *Nature* **374**, 555–559 (1995).
13. Lu, H. P., Xun, L. & Xie, X. S. Single-molecule enzymatic dynamics. *Science* **282**, 1877–1882 (1998).
14. Flomenbom, O. et al. Stretched exponential decay and correlations in the catalytic activity of fluctuating single lipase molecules. *Proc. Natl Acad. Sci. USA* **102**, 2368–2372 (2005).
15. Wiita, A. P. et al. Probing the chemistry of thioredoxin catalysis with force. *Nature* **450**, 124–127 (2007).
16. Schoen, I., Hu, W., Klotzsch, E. & Vogel, V. Probing cellular traction forces by micropillar arrays: contribution of substrate warping to pillar deflection. *Nano Lett.* **10**, 1823–1830 (2010).
17. Bustamante, C., Cheng, W. & Mejia, Y. X. Revisiting the central dogma one molecule at a time. *Cell* **144**, 480–497 (2011).
18. Li, G.-W. & Xie, X. S. Central dogma at the single-molecule level in living cells. *Nature* **475**, 308–315 (2011).
19. Grossman-Haham, I., Rosenblum, G., Namani, T. & Hofmann, H. Slow domain reconfiguration causes power-law kinetics in a two-state enzyme. *Proc. Natl Acad. Sci. USA* **115**, 513–518 (2018).
20. Kou, S. C., Cherayil, B. J., Min, W., English, B. P. & Xie, X. S. Single-molecule Michaelis–Menten equations. *J. Phys. Chem. B* **109**, 19068–19081 (2005).
21. English, B. P. et al. Ever-fluctuating single enzyme molecules: Michaelis-Menten equation revisited. *Nat. Chem. Biol.* **2**, 87–94 (2006).
22. Min, W. et al. When does the Michaelis–Menten equation hold for fluctuating enzymes? *J. Phys. Chem. B* **110**, 20093–20097 (2006).
23. Cao, J. Michaelis–Menten equation and detailed balance in enzymatic networks. *J. Phys. Chem. B* **115**, 5493–5498 (2011).
24. Kolomeisky, A. B. Michaelis–Menten relations for complex enzymatic networks. *J. Chem. Phys.* **134**, 155101–155106 (2011).
25. Xie, X. S. Enzyme kinetics, past and present. *Science* **342**, 1457–1459 (2013).
26. Singh, D. & Chaudhury, S. Statistical properties of fluctuating enzymes with dynamic cooperativity using a first passage time distribution formalism. *J. Chem. Phys.* **146**, 145103–145107 (2017).
27. Moffitt, J. R. & Bustamante, C. Extracting signal from noise: kinetic mechanisms from a Michaelis–Menten-like expression for enzymatic fluctuations. *FEBS J.* **281**, 498–517 (2014).
28. Chemla, Y. R., Moffitt, J. R. & Bustamante, C. Exact solutions for kinetic models of macromolecular dynamics. *J. Phys. Chem. B* **112**, 6025–6044 (2008).
29. Moffitt, J. R., Chemla, Y. R. & Bustamante, C. Mechanistic constraints from the substrate concentration dependence of enzymatic fluctuations. *Proc. Natl Acad. Sci. USA* **107**, 15739–15744 (2010).
30. Chaudhury, S., Cao, J. & Sinitsyn, N. A. Universality of Poisson indicator and fano factor of transport event statistics in ion channels and enzyme kinetics. *J. Phys. Chem. B* **117**, 503–509 (2013).
31. Moffitt, J. R. et al. Intersubunit coordination in a homomeric ring ATPase. *Nature* **457**, 446–450 (2009).
32. Yu, J., Moffitt, J., Hetherington, C. L., Bustamante, C. & Oster, G. Mechanochemistry of a viral DNA packaging motor. *J. Mol. Biol.* **400**, 186–203 (2010).

33. Edman, L. & Rigler, R. Memory landscapes of single-enzyme molecules. *Proc. Natl Acad. Sci. USA* **97**, 8266–8271 (2000).
34. Berezhkovskii, A. M. & Makarov, D. E. Single-molecule test for Markovianity of the dynamics along a reaction coordinate. *J. Phys. Chem. Lett.* **9**, 2190–2195 (2018).
35. Song, K., Makarov, D. E. & Vouga, E. Compression algorithms reveal memory effects and static disorder in single-molecule trajectories. *Phys. Rev. Res.* **5**, L012026 (2023).
36. Jung, W., Yang, S. & Sung, J. Novel chemical kinetics for a single enzyme reaction: relationship between substrate concentration and the second moment of enzyme reaction time. *J. Phys. Chem. B* **114**, 9840–9847 (2010).
37. Yang, S., Cao, J., Silbey, R. J. & Sung, J. Quantitative interpretation of the randomness in single enzyme turnover times. *Biophys. J.* **101**, 519–524 (2011).
38. Reuveni, S., Urbakh, M. & Klafter, J. Role of substrate unbinding in Michaelis–Menten enzymatic reactions. *Proc. Natl Acad. Sci. USA* **111**, 4391–4396 (2014).
39. Rotbart, T., Reuveni, S. & Urbakh, M. Michaelis-Menten reaction scheme as a unified approach towards the optimal restart problem. *Phys. Rev. E* **92**, 060101 (2015).
40. Robin, T., Reuveni, S. & Urbakh, M. Single-molecule theory of enzymatic inhibition. *Nat. Commun.* **9**, 779 (2018).
41. Klafter, J. & Sokolov, I. M. *First Steps in Random Walks: From Tools to Applications* (Oxford University Press, 2011).
42. Singh, D., Punia, B. & Chaudhury, S. Theoretical tools to quantify stochastic fluctuations in single-molecule catalysis by enzymes and nanoparticles. *ACS Omega* **7**, 47587–47600 (2022).
43. Li, X. & Kolomeisky, A. B. Mechanisms and topology determination of complex chemical and biological network systems from first-passage theoretical approach. *J. Chem. Phys.* **139**, 144106–144109 (2013).
44. Li, X., Kolomeisky, A. B. & Valleriani, A. Pathway structure determination in complex stochastic networks with non-exponential dwell times. *J. Chem. Phys.* **140**, 184102–184106 (2014).
45. Thorneywork, A. L. et al. Direct detection of molecular intermediates from first-passage times. *Sci. Adv.* **6**, eaaz4642 (2020).
46. Singh, D., Urbakh, M. & Reuveni, S. Inferring binding rates from enzymatic turnover time statistics. *bioRxiv* https://doi.org/10.1101/2025.02.04.636412 (2025).

Acknowledgements

This project has received funding from the European Research Council (ERC) under the European Union's Horizon 2020 research and innovation program (grant agreement No. 947731, S.R.).

Author contributions

D.S. and T.R. derived analytical results. D.S. performed numerical simulations. M.U. and S.R. designed and supervised the research. D.S., M.U., and S.R. wrote the manuscript.

Competing interests

The authors declare no competing interests.

Additional information

Supplementary information The online version contains supplementary material available at https://doi.org/10.1038/s41467-025-57327-2.

Correspondence and requests for materials should be addressed to Shlomi Reuveni.

Peer review information *Nature Communications* thanks Hideshi Ooka and Daniel Weilandt for their contribution to the peer review of this work. A peer review file is available.